Modeling of Wiggler Fields for Tracking.

M. Venturini
LBNL

Outline

- From numerical field maps to field representations suitable for tracking. A short survey.
  - Emphasis on 3D multipole field representation.

- Tools for integration of equations of motion and assessment of dynamical effects of wigglers.

- Impact of wiggler nonlinearities on ILC damping ring lattices.

Cylindrical or Cartesian coordinates for field representation?

The Cartesian way.

- Simple modeling of wigglers has a more natural representation in Cartesian basis functions - e.g. `Halbach' approximation :

$$B_x = -B_0 \frac{k_x}{k_y} \sin(k_x x) \sinh(k_y y) \cos(k_z z)$$

$$B_y = B_0 \cos(k_x x) \cosh(k_y y) \cos(k_z z)$$

$$B_z = -B_0 \cos(k_x x) \sinh(k_y y) \sin(k_z z)\, k_z$$

- In general fields from actual devices are poorly represented by one mode. Make this representation general by summing over all modes.
- Several coefficients in expansion have to be used for accurate representation of actual fields.
- Note: for simulation of dynamics an analytic field representation is preferable to interpolation of numerical field map on grid.

Determine coefficients of field representation

- One field component on boundary of 3D empty region determines uniquely full magnetic field within that region.
- However, if mid-plane symmetry holds, knowledge of B_y on a plane parallel to (preferable) or on the mid-plane is sufficient.

- At least two ways to obtain coefficients for field representation:
  - by Fourier transform
  - by fitting

Coefficients from FT Inversion

- Scalar potential solving Laplace equation:

$$\Psi = \sum_{\ell,n} c_{n,\ell} \cos(nk_x x)\sin(\ell k_z z)\cosh(k_y y)$$

with $\quad k_x = 2p / L_x,\ k_z = 2p / L_z\,,$

$$k_y^2 = n^2 k_x^2 + \ell^2 k_z^2$$

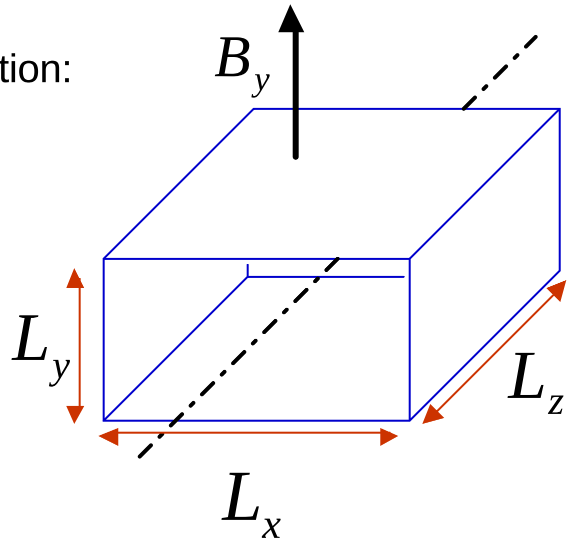

$$B_y = \sum_{\ell,n} c_{n,\ell} k_y \cos(nk_x x)\sin(\ell k_z z)\sinh(k_y y)$$

$$\boxed{c_{n,\ell} = \frac{2}{L_x}\int_{-L_x/2}^{L_x/2} dx\, \frac{2}{L_z}\int_{-L_z/2}^{L_z/2} dx\, \sin(\ell k_z z)\cos(nk_x x) B_y^{data}(x, y = L_y)}$$

Coefficients of field representation **Magnetic field data**

If possible use field data far from midplane

$$B_y^{data} = \sum_{\ell,n} c_{n,\ell}^{data} \cos(nk_x x)\sin(\ell k_z z)$$

$$\boxed{c_{n,\ell} = \frac{c_{\ell,n}^{data}}{\cosh(k_y L_y / 2)}}$$

Notice denominator grows with mode numbers if L_y does not vanish.

The larger L_y the better.

$recall \quad k_y^2 = n^2 k_x^2 + \ell^2 k_z^2$

- FT method is fast.
- However, Fourier transforming in x in unnatural as fields are not periodic. From F-series to F- integrals.
- Fields are usually not known over a large span of support L_x. For finite L_x convergence in Fourier space is slow. A large number of modes needed to get accuracy

Coefficients from fitting

- Accuracy can be improved by regarding coefficients of Fourier expansions as free parameters to be fitted against values of numerical field map in selected points (or the entire 3D grid – if available).
- Method can be accurate.
- D. Sagan *et al*. found rms residual field error from fitting of the order of ~9 Gauss (~2 T peak field) for CESR wigglers.
- For good results reliable optimization routines are needed.
- Procedure can be time consuming.

Field data vs. fit for CESR wiggler
(D. Sagan *et al*., PAC03**)**

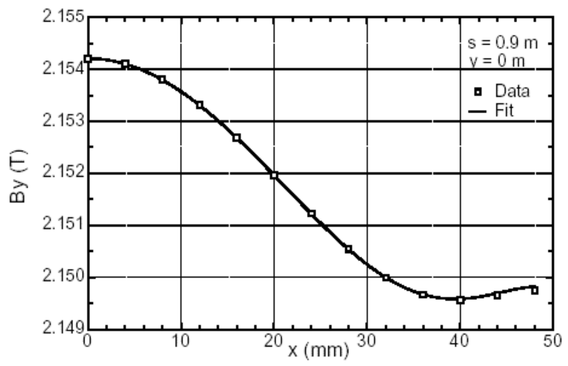

A case for representation of fields in cylindrical coordinates

- Using a field representation in terms of cylindrical basis functions (*i.e.* 3D multipole expansion)

- Determine coefficients by Fourier transform.

- A few advantages:
  - Faster and simpler than fitting.
  - Accurate (natural periodicity in azimuthal coordinate).
  - Uses language closer to familiar (2D) multipole field representation for conventional magnets.

Basic formulas

- Scalar potential solving Laplace equation in cylindrical variables

$$\boxed{\Psi = \sum_{m,\ell} I_m(\ell k_z r)\sin(\ell k_z z)\left[b_{m,\ell}\sin(mj) + a_{m,\ell}\cos(mj)\right]}$$

modified Bessel function

skew components

normal components

- (normal) magnetic field components

$$B_r = \sum_{m,\ell} \ell k_z b_{m,\ell} I_m^{'}(\ell k_z r)\sin(mj)\sin(\ell k_z z)$$

$$B_j = \sum_{m,\ell} m b_{m,\ell} I_m(\ell k_z r)\cos(mj)\sin(\ell k_z z)$$

$$B_z = \sum_{m,\ell} \ell k_z b_{m,\ell} I_m(\ell k_z r)\sin(mj)\cos(\ell k_z z)$$

Alternate expression: introduce the generalized gradients

- Expand modified Bessel function in power series in radial variable; carry out sum over longitudinal modes:

$$\boxed{\Psi = \sum_{m,\ell} (-1)^{\ell} b_{m,\ell} \frac{m!}{2^{2\ell}\, \ell!(\ell+m)!} C_m^{[2\ell]}(z)\, r^{2\ell+m} \sin(m j)}$$

Generalized gradients and *2l*-derivatives

- The $C_m^{[2l]}(z)$ can be arbitrary - Ψ will still satisfy Laplace equation

$$B_r = \left(C_1(z) - \frac{3}{8} r^2 C_1^{[2]}(z) + \frac{5}{192} r^4 C_1^{[4]}(z) + \dots \right) \sin(j) +$$

dipole

$$\left(2C_2(z) r - \frac{1}{6} r^3 C_2^{[2]}(z) + \dots \right) \sin(2j) +$$

quadrupole

$$\left(3C_3(z) r^2 - \frac{5}{16} r^4 C_3^{[2]}(z) + \dots \right) \sin(3j) + \dots (\sin \leftrightarrow \cos)$$

sextupole

From magnetic field data on cylindrical surface to the generalized gradients

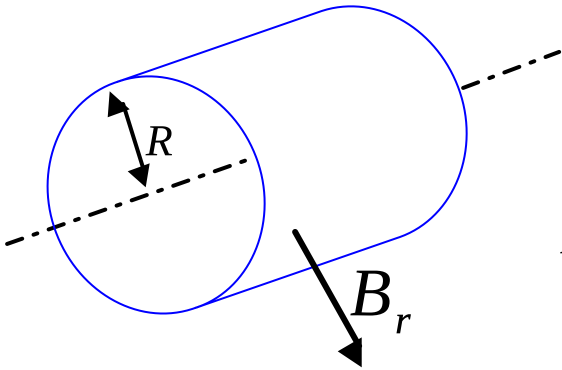

$$B_r(r = R, j, z) = \sum_{m=1} B_m(R, z)\sin(mj)$$

Data on cylinder

$$B_m(R, z) = \frac{1}{p}\int_0^{2p} dj\, \sin(mj) B_r(R, j, z)$$

Fourier integral on ϕ

$$\overline{B_{m,p}} = \frac{1}{l_w}\int_0^{l_w} dz\, e^{-2pipz/l_w} B_m(R, z)$$

Fourier integral on z

$$C_m^{[k]}(z) = \frac{1}{2^m m!}\sum_{p=-\infty}^{\infty} i^k \left(\frac{2pp}{l_w}\right)^{m+k-1} \frac{\overline{B_{m,p}}}{I_m'(2ppR/l_w)} e^{2pipz/l_w}$$

Generalized gradients and derivatives

Smoothing properties of method

$$C_m^{[k]}(z) = \frac{1}{2^m m!} \sum_{p=-\infty}^{\infty} i^k \left(\frac{2pp}{l_w} \right)^{m+k-1} \frac{\overline{B_{m,p}}}{I_m^{'}(2ppR/l_w)} e^{2pipz/l_w}$$

Low pass filter

- Modified Bessel function grows **exponentially** for large arguments.

- Term with Bessel function acts as a **filter** that dampens high frequency components (possibly due to numerical random noise) of magnetic field data.

- Caution: this natural filtering is going to make efficient use of good numerical field data. It won’t fix bad numerical data.

From cylindrical back to Cartesian …

- Fourier analysis is more naturally done using cylindrical coordinate basis functions.
- Still, one may desire to have field expansions in Cartesian coordinate basis functions.
- Conversion can be done between coefficients of two series. For a purely normal field:

$$\boxed{c_{n,\ell} = -\frac{1}{k_y^2 \cosh(k_y R)} \sum_{p=0} (-1)^{2p+1} \ell k_z b_{2p+1,\ell} I'_{2p+1}(\ell k_z r)}$$

$$k_x = 2p \,/\, L_x,\; k_z = 2p \,/\, L_z\,,\;\; \mathit{witharbitrarily\ fixed}\; L_x, L_y$$

$$k_y^2 = n^2 k_x^2 + \ell^2 k_z^2$$

- Our experience shows this is more accurate than working all the way in Cartesian coordinates from the start.

…and from Cartesian to cylindrical

- One can also express coefficients of the series in cylindrical coordinate basis in terms of those in the Cartesian basis series.
- Example: infinitely wide wiggler with one longitudinal harmonic

$$B_x = 0$$
$$B_y = B_0 \cos(kz)\cosh(ky)$$
$$B_z = -B_0 \sin(kz)\sinh(ky)$$

- Generalized gradients:

$$C_m(z) = B_0 \cos(kz) k^{m-1} \frac{(-1)^{\frac{m-1}{2}}}{2^{m-1} m!}, \quad for\ odd\, m;\ C_m = 0\ otherwise$$

- Infinite spectrum of multipoles is present (dynamics is trivial in x but not in y where there are linear and nonlinear effects)

- Two examples of 3D multipole analysis:
  - CESR 8-pole wiggler
  - LBL design for NLC-MDR wiggler (one period)

Analysis of field map for CESR 8-pole wigglers

- Very nice numerical field map available.
- Calculated using Opera, Mermaid (J. Crittenden *et al*.,PAC03).
- Courtesy of Rubin *et al.* from Cornell.

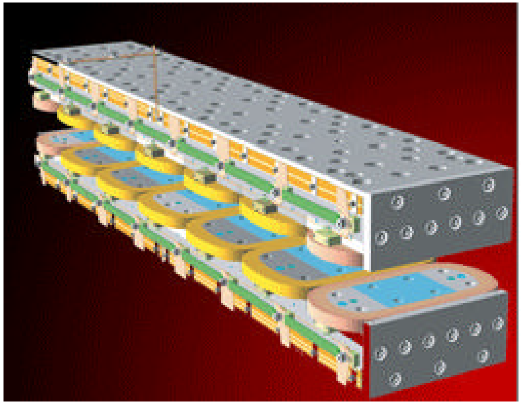

7-pole wiggler

Dipole field harmonic at ***R=2.6 cm***

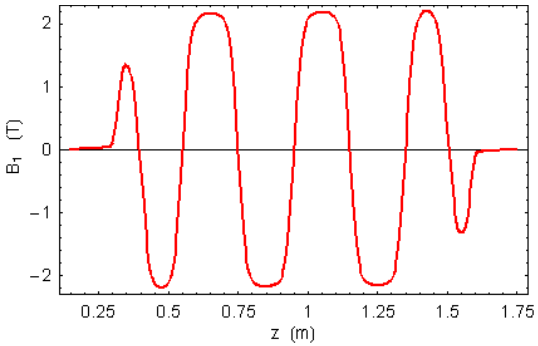

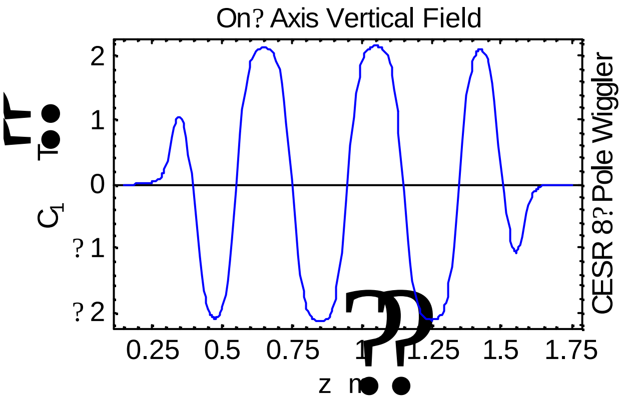

Accuracy of field representation (I)

- On surface of cylinder of radius R=2.6 cm residual from 3D multipole representation truncated through 14-pole is 1 Gauss or less.

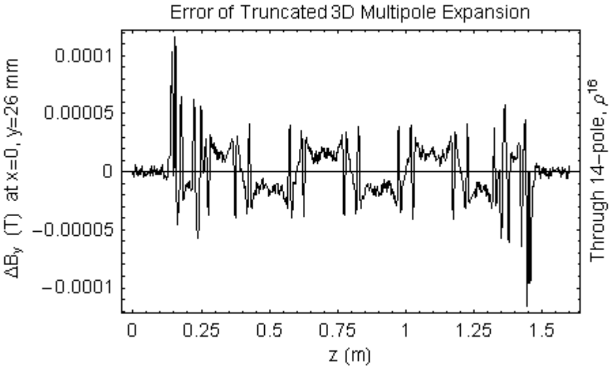

- Within cylinder field residual becomes smaller (as expected).
- Large errors at wiggler ends are due to discontinuous termination of field data. They can be easily fixed by extending fields in z making them periodic.

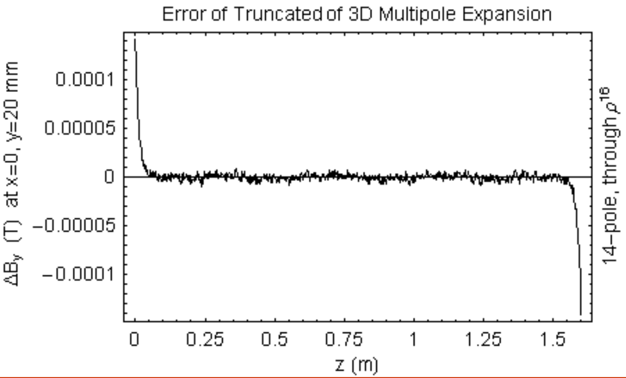

Accuracy of field representation (II)

- Accuracy of field representation is an indicator of numerical quality of the field map.
- Invariance of results against variations of selected radius of cylindrical surface for data analysis is also a useful test.

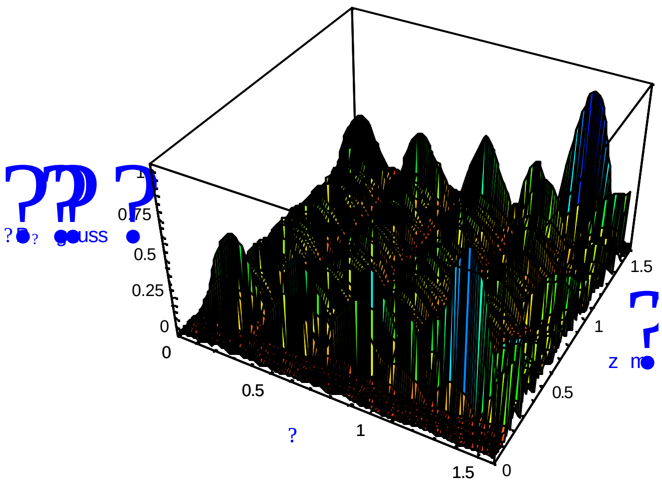

on cylinder of radius ***R=2.6 cm***

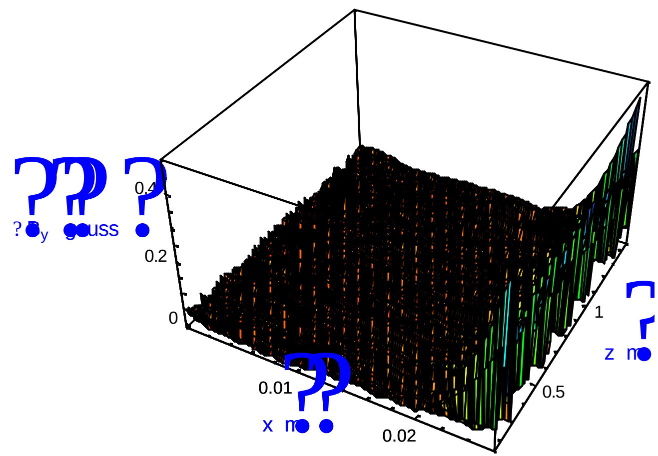

on ***x-y*** plane

CESR 8-pole wigglers: Field quality

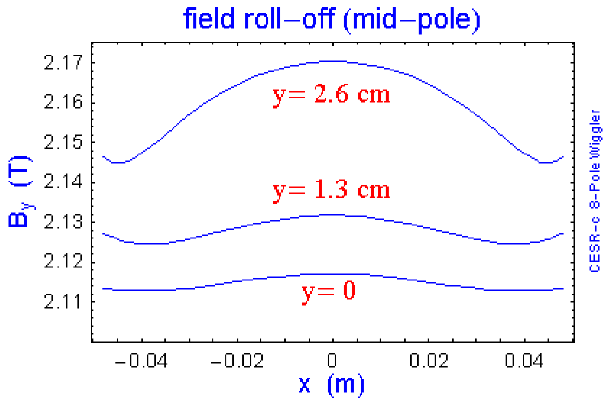

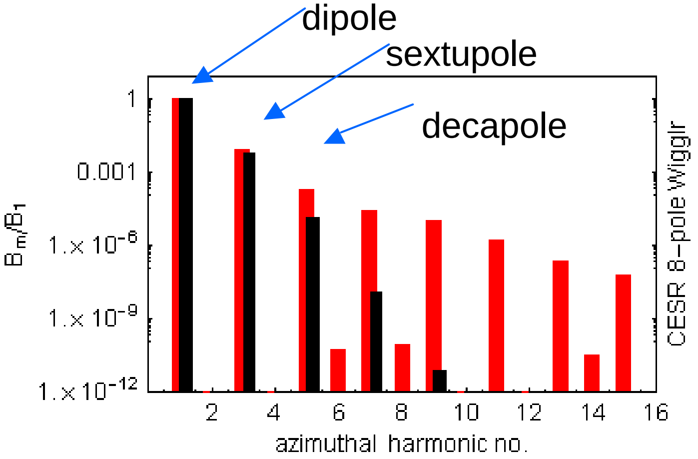

- **Red bars**: spectrum of multipole field integrated over half a period
- **Black bars:** spectrum for infinitely wide wiggler

- Ultimately the field quality is decided by the dynamical effects on the beam

CESR 8-pole wigglers: generalized gradients

4th derivative of on-axis field

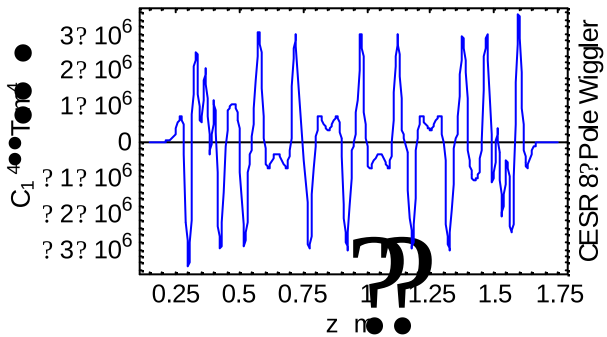

Decapole gradient

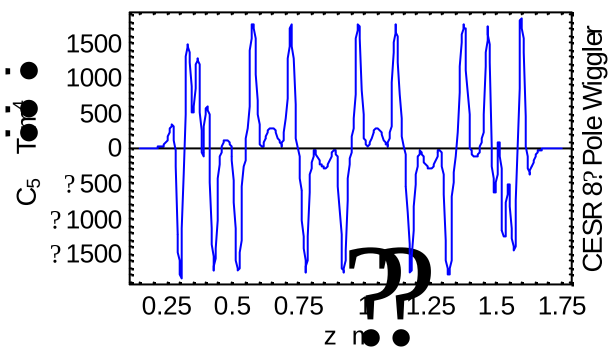

Sextupole gradient and 2nd derivative of on-axis field

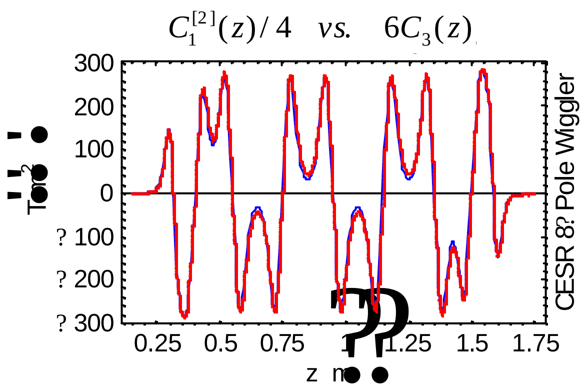

In infinitely wide wiggler:

$$C_1^{[2]}(z)/4 = 6C_3(z)$$

Model for NLC-MDR wiggler (one period)

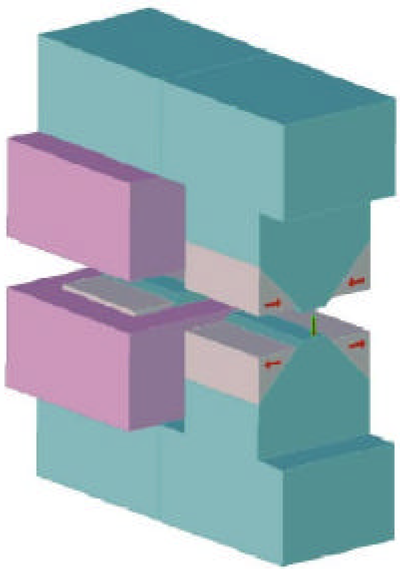

Figure 1. Electromagnet wiggler, one period.

- Main design parameters:

$$B_{w0} = 2.15\ T$$
$$l_w = 0.27\ m$$
$$pole\ gap = 2\,cm$$

- A model of wiggler design for NLC damping ring was developed at LBL (J. Corlett *et al*., LBL-CBP Tech. Note 199).
- Several 1-period 3D field maps with increasing numerical quality have been produced.
- This model was used in the past for the NLC-MDR studies and in now being used in some of the tracking for the ILC DR.

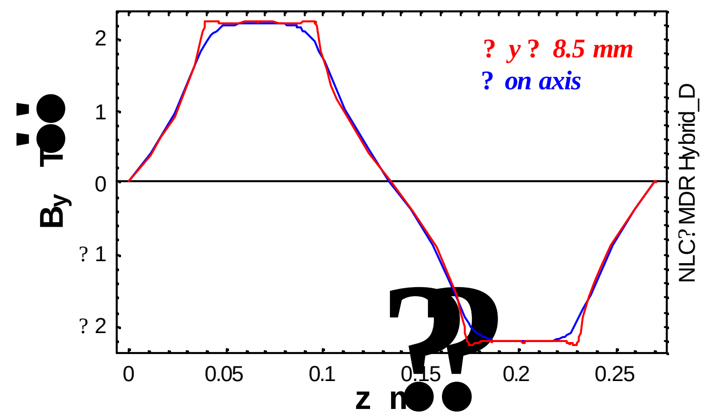

NLC-MDR wiggler model: accuracy of field representation / numerical quality of field map

- Numerical quality of best field data available is still not very high but improved from first field map produced. Still, it may be acceptable.
- Peak error from field representation ~15 Gauss

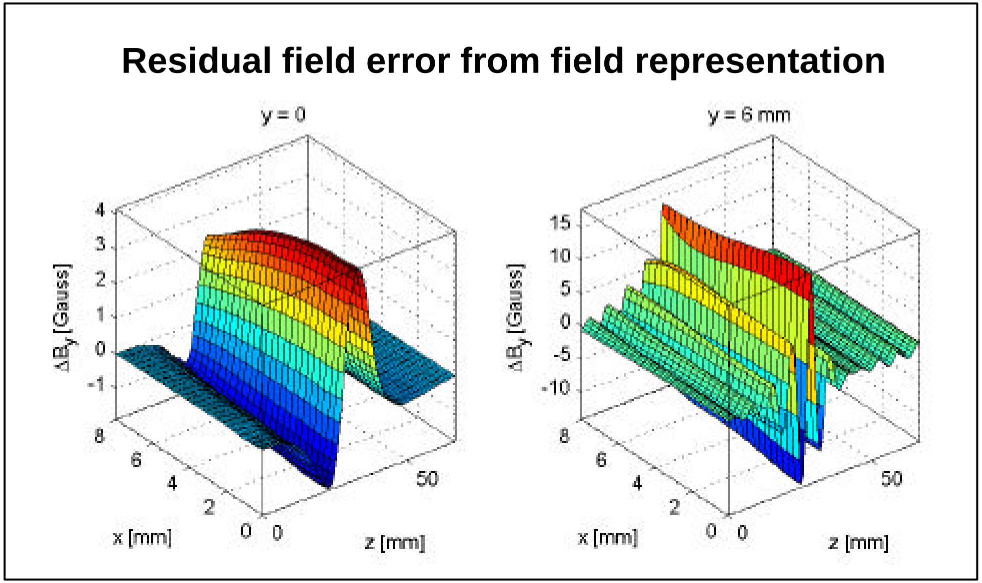

NLC-MDR wiggler model: field quality

Comparison between field roll-offs

NLC-MDR w-prototype

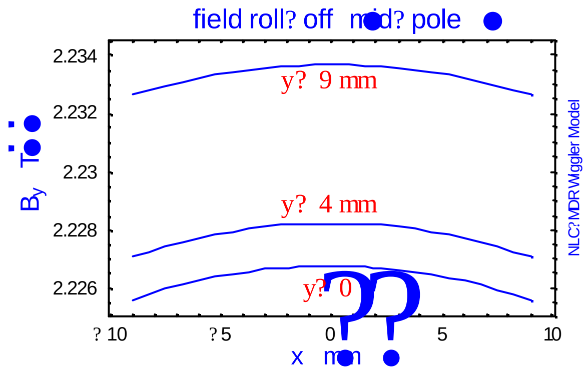

CESR 8w

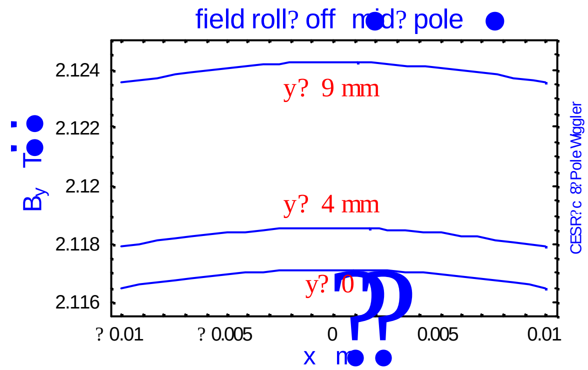

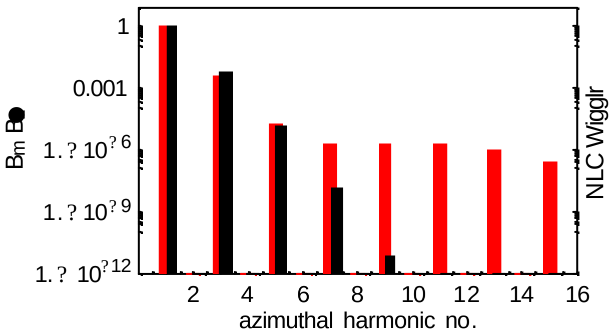

Integrated multipole spectrum

div B=0 as an additional indicator of numerical quality of field data

CESR 8-pole w

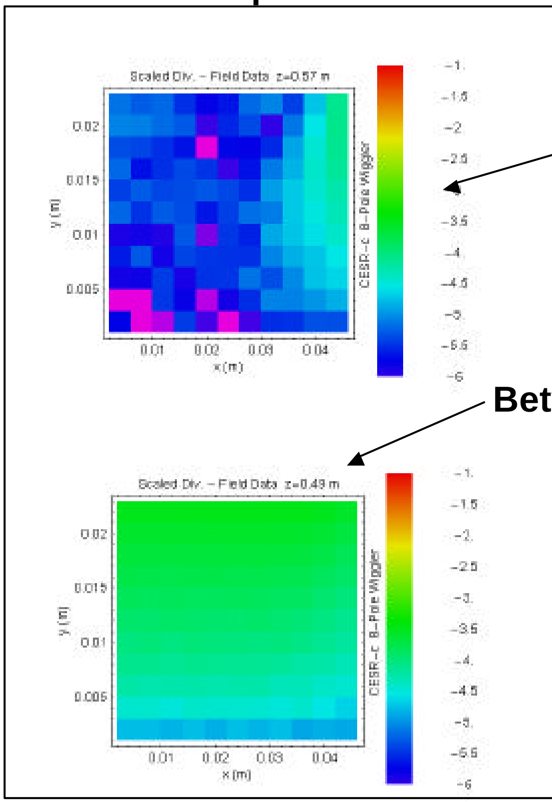

NLC-MDR w (worst case of produced field map)

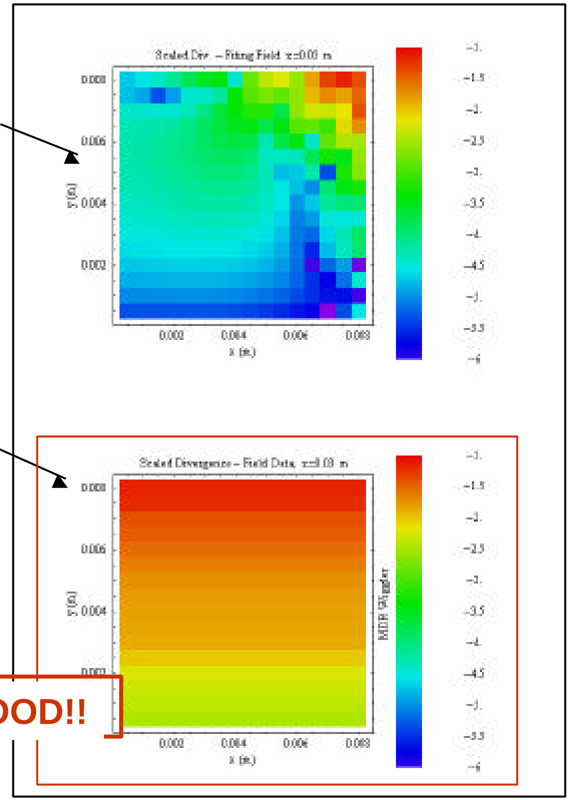

Midpole

Between poles

NOT GOOD!!

Integration of Eq.'s of motion thru wigglers

- To do tracking: integrate equation of motion
  - for individual particles through a desired order in time step (possibly using a symplectic integrator).
  - for the transfer map through a given order in the transverse variables. Transfer map is expressed in terms of the deviation variables from reference orbit (our choice).

- At LBL we've been using two sets of tools
  - **Merlin/Cosy** (Cosy for calculation transfer map in Taylor; Merlin for tracking and motion analysis). Field representation in Cartesian variables in equations of motion obtained by conversion from coefficients of the series cylindrical representation. Symplectic/nonsymplectic tracking.
  - **MaryLie** - for both Lie map production and symplectic tracking using method of generating functions (3rd order in transverse variables). Cylindrical representation of fields is used at input.

Example – Computation of transfer functions for CESR 8-pole wigglers

Reference Orbit

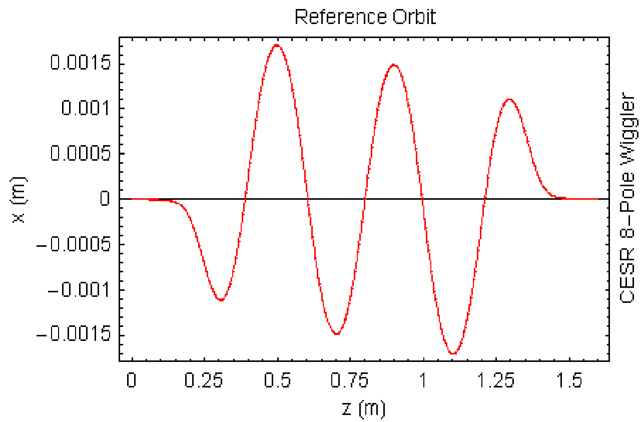

Horizontal plane kicks

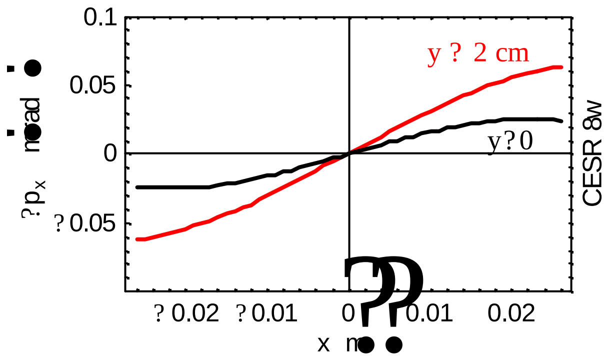

Vertical plane kicks

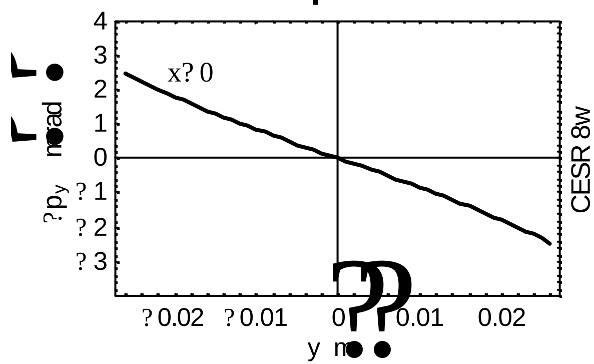

- Transfer map for wiggler is calculated relative to the reference orbit.
- Calculation done with MaryLie

Cross-validation of numerical tools

- **MaryLie** vs. **Merlin/Cosy**.
- Comparison of transfer maps (Taylor form) for wiggler period
- Maps through 3rd order.
- NLC MDR wiggler model.

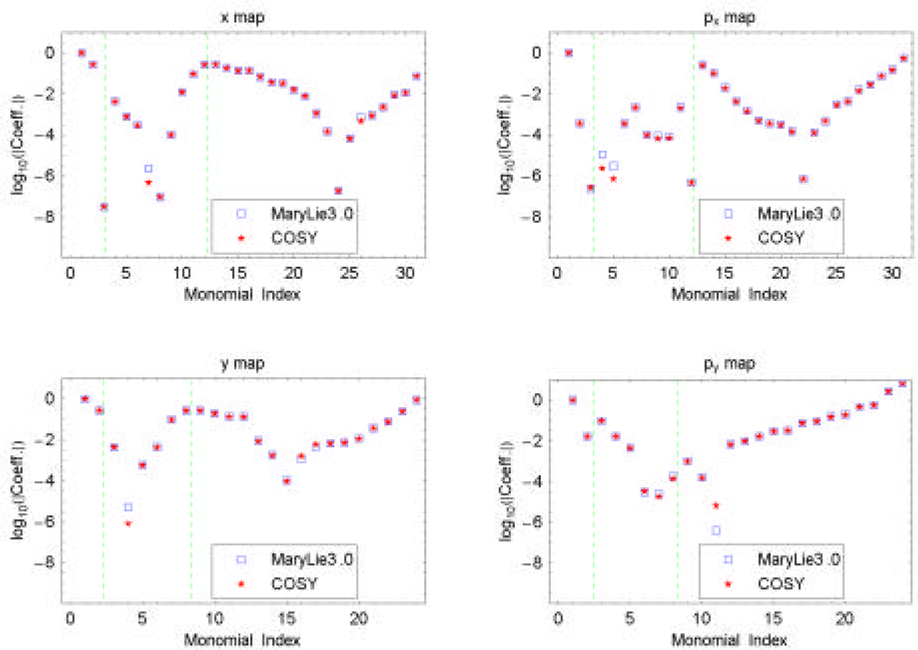

Simplified kicks through one wiggler period in terms of generalized gradients

- Assume kick approximation ($X,Y=const$) through wiggler period. Fields with mid-plane symmetry.
- Momentum kick in vertical plane through 3rd order in Y, 1st-order in amplitude of reference orbit:

$$\Delta p_Y \approx \frac{1}{Brho}\int_0^{l_w}\left(B_x(x^r(z),Y,z)-\tfrac{dx^r}{sz}B_z(x^r(z),Y,z)\right)dz$$

$$\Delta p_Y = Y\left(\Delta p_Y\right)_1 + Y^3\left(\Delta p_Y\right)_3$$

sextupole feed-down

dipole

$$\left(\Delta p_Y\right)_1 = \frac{1}{Brho}\int_0^{l_w} dz\, x^r(z)\left(6C_3(z)+\frac{3}{4}C_1^{[2]}(z)\right) = \frac{1}{Brho}\int_0^{l_w} dz\, x^r(z)6C_3(z) - \frac{1}{Brho}\frac{3}{4}\int_0^{l_w} dz\left[C_1^{[1]}(z)\right]^2$$

$$\left(\Delta p_Y\right)_3 = -\frac{1}{Brho}\int_0^{l_w} dz\, x^r(z)\left(20C_5(z)+\frac{5}{4}C_3^{[2]}(z)+\frac{5}{48}C_1^{[4]}(z)\right)$$

decapole feed-down

sextupole feed-down

dipole

Dipole field component is always focusing. Use

$$\frac{d^2x^r}{dz^2} \approx -\frac{1}{Brho}C_1(z)$$

Purely horizontal kicks

- 3rd order horizontal kick $\Delta p_X \approx \frac{c}{Brho}\int_0^{l_w} B_y(x^r(z)+X,0,z)\,dz$

$$\Delta p_X = X(\Delta p_X)_1 + X^3(\Delta p_X)_3$$

$$(\Delta p_X)_1 = -\frac{1}{Brho}\int_0^{l_w} dz\, x^r(z)\left(6C_3(z)-\frac{1}{4}C_1^{[2]}(z)\right) = -\frac{6}{Brho}\int_0^{l_w} dz\, x^r(z) C_3(z) - \frac{1}{4Brho}\int_0^{l_w} dz\,\left[C_1^{[1]}(z)\right]^2$$

$$(\Delta p_X)_3 = -\frac{1}{Brho}\int_0^{l_w} dz\, x^r(z)\left(20C_5(z)-\frac{3}{4}C_3^{[2]}(z)+\frac{1}{48}C_1^{[4]}(z)\right)$$

Always focusing

- Consistency check: kick vanishes (order by order) when $C_m(z)$ is from infinitely wide wiggler.
- Decapole feed-down term to 3rd order kick has the radial dependency and azimuthal symmetry of kick from a real octupole magnet.
  - this is general e.g. 14-pole feed-down to 5th order kick has the azimuthal & radial kick from a duodecapole, etc.
  - If these terms are dominant in kick one can hope to compensate wiggler nonlinearities locally with standard multipole magnets (effectively, this is what was done in the SPEAR BL11 wiggler insertions).
- Notice that a wiggler consisting of purely dipole field $C_3(z)= C_5(z)=\ldots 0$ would have linear focusing in both x and y.

Tracking through ILC-DR lattices

- DA aperture is an issue with ILC-DR lattices. Dominant nonlinearities are from chromatic sextupoles.

- Wiggler nonlinearities appear to play a smaller role but should be kept under control.

- Impact of wiggler nonlinearities on wiggler design. Two examples considered:
  - 6Km ILC-DR [lattice design by FNAL team *(A. Xiao (July 04), Mishra et al. (Oct. 04)],* with NLC-MDR LBL wiggler prototype. Wiggler ends modeled using bends. Impact of wigglers is modest.

  - TESLA-DR dog-bone lattice with TESLA wiggler prototype. (Wiggler ends also modeled using bends). Field map courtesy of W. Decking.
    Impact of wiggler is substantial.

6 Km FNAL DR (nonlinear wigglers)

Frequency map in x/y plane

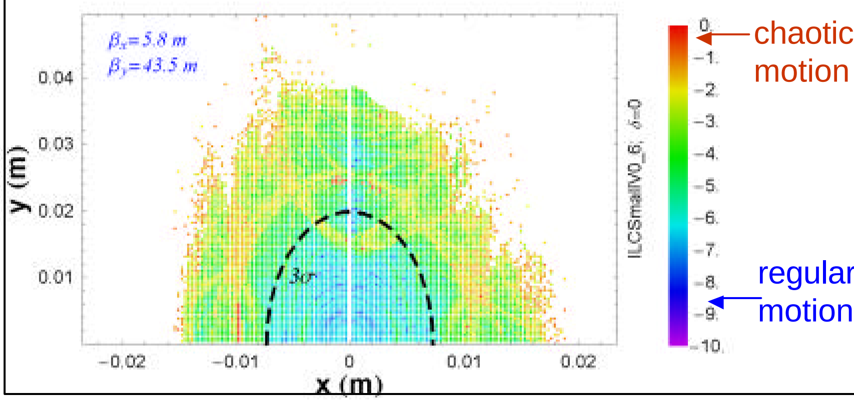

Frequency map in tune space

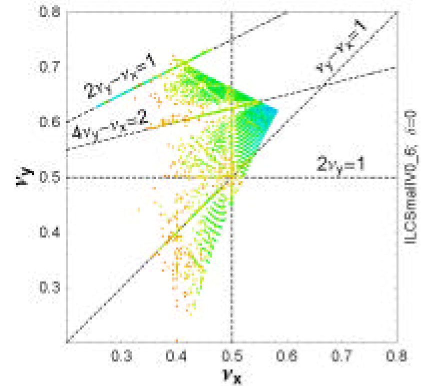

Identify resonances in x/y plane

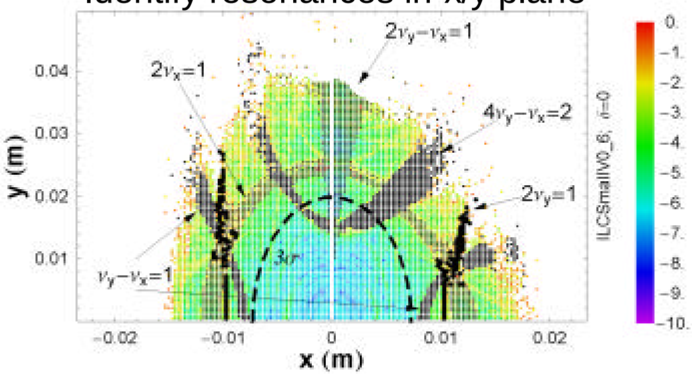

Frequency maps measure diffusion in tune; allow identification of resonances that may be affecting the DA.

- Bluer orbits have more regular motion.
- Reddish orbits are chaotic.

- Short term tracking done with MaryLie3.0
- Error-free lattice

6 Km FNAL DR (NL *vs*. linear wigglers)

On-momentum wiggler nonlinearities cause noticeable but modest but DA reduction.

Nonlinear wigglers

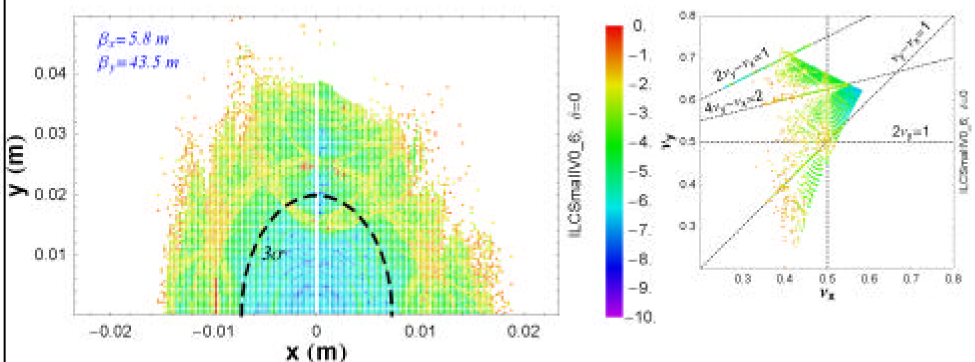

Linear wigglers

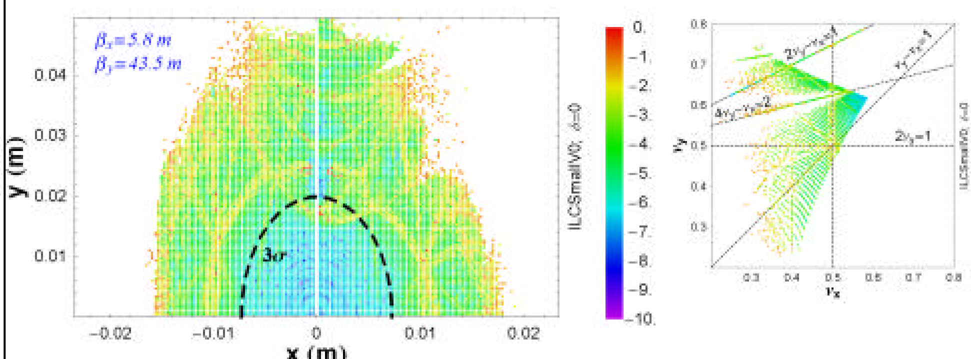

Anharmonicities are within 10-20 %

	Linear*	NL*
$\partial\nu_x / \partial J_x$	-3977.	-3434.
$\partial\nu_y / \partial J_y$	2593.	3136
$\partial\nu_x / \partial J_y$	-6644.	-6379.

*in units of m^{-1}

TESLA 17km DR

Linear wigglers

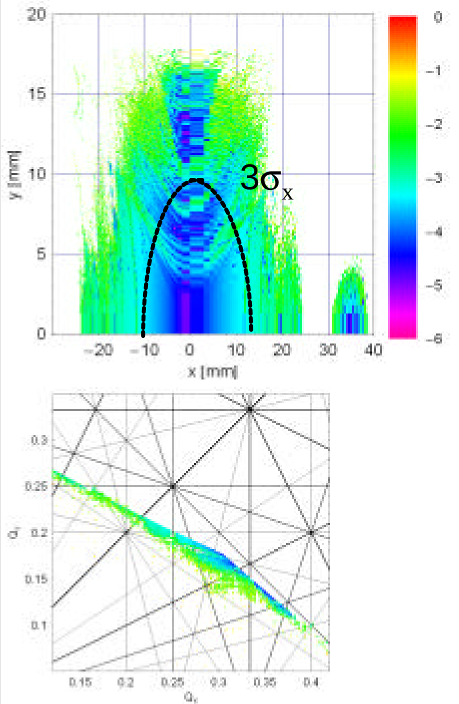

Nonlinear wigglers

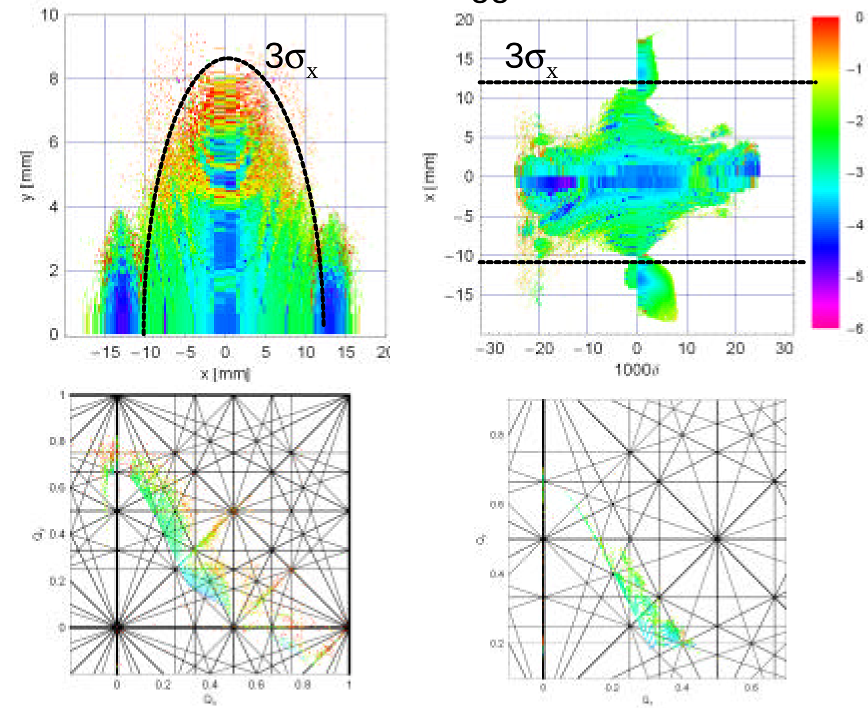

Wiggler map calculation/tracking done with Cosy/Merlin by A. Wolski

betax=15.4 m; betay=8.6 m
At inj.: σ_x =3.9 mm; σ_y =3 mm

DA and transfer functions: NLC MDR *vs.* TESLA DR wiggler

- Nonlinearities for model of TESLA wigglers are considerably larger than those from the NLC wiggler model.
- Relative strong feed-down from decapole field component present in TESLA wiggler.

Transfer functions for 1 period

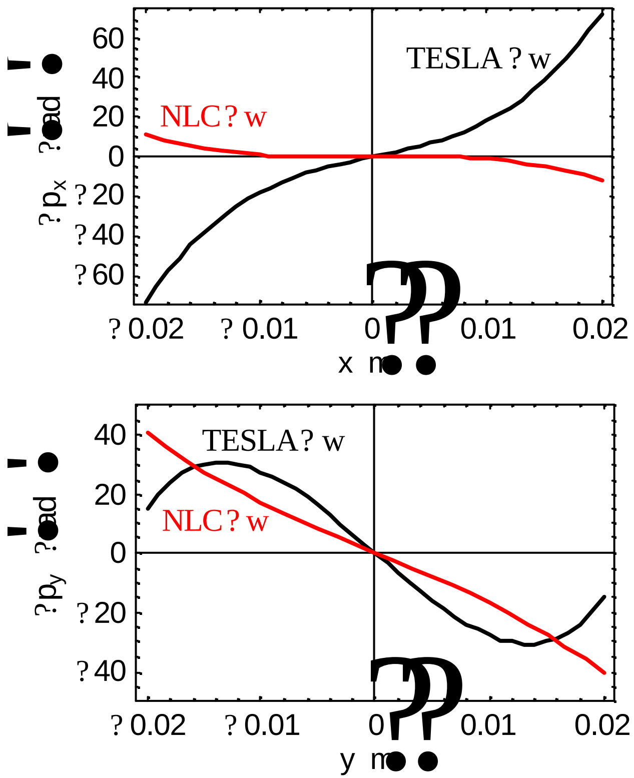

Conclusions

- A 3D multipole (cylindrical representation) of fields with coefficients obtained by FT is fast to compute, simple and accurate.

- Cross-validated set of tools for calculation of dynamics including linear and nonlinear effects. It would be desirable to extend validations against codes from other groups.

- Results from tracking of ILC lattices confirms that field quality in wigglers does have an impact on dynamic aperture. Wiggler design should be tuned to tame nonlinearities.